

PREDICTION OF LOAD - DEFORMATION BEHAVIOR AND LOAD CARRYING CAPACITY OF PILES IN SAND

Abdul Muqtadir¹ and Jahangir Morshed²

ABSTRACT : A nonlinear incremental finite element procedure is developed for the analysis of axially loaded piles in sand. In this procedure, the pile shaft is idealized using beam column elements and the soil is modelled as a series of unconnected nonlinear springs. Initial spring stiffness of the frictional and tip resistance are modelled using t-z and p-z subgrade reaction respectively; the t-z concept was proposed by Kraft et. al., and p-z concept was proposed by Randolph and Worth. The non linearity of spring stiffness are captured using the Ramberg-Osgood model. The procedure thus developed is applied in predicting load-deformation behavior, failure loads and axial load distribution of the piles. Finally, the predicted values are compared with the model test results.

KEY WORDS : Nonlinear analysis, failure loads, t-z and p-z concepts, model test, displacement and non-displacement piles.

INTRODUCTION

Prediction of load-deformation response of piles is difficult. The pile load test is considered to be one of the most reliable methods for predicting the load-deformation response. However, this test is both time-consuming and expensive. Alternatively, it is more advantageous to develop simple analytical methods based on limited test results. In this study, a simple analytical method for predicting the nonlinear load-deformation response of an axially loaded pile in sand is presented. The method is based on one-dimensional finite element idealization of pile-soil system. The soil is idealized as a series of independent springs (Winkler 1867). The nonlinear behavior of soil is simulated using the Ramberg-Osgood model (Desai and Wu 1976). The method includes an empirical procedure to determine the parameters of the Ramberg-Osgood model. In the empirical procedure, the shear resistance along the pile length is modeled using the t-z concept of Kraft et al. (1981), and the tip resistance at the pile base is modeled using the p-z concept of Randolph

1 Department of Civil Engineering, BUET, Dhaka-1000, Bangladesh

2 Department of Civil Engineering, University of Utah, Logan, USA

and Wroth (1978). The validity of the present method is checked with model test results.

DETAILS OF MODEL PILE TESTS

Characterization of Sand

A loose to medium dense sand was used for the model test (Siddique 1988 and Muqtadir et. al 1990). The sand was uniformly graded with a uniformity coefficient (C_U) of 1.15. It had an effective grain size diameter (D_{60}) of 0.013 cm. The sand had a specific gravity of 2.65 and an internal friction angle of 31° .

DESCRIPTION OF PILES

Three model piles were tested. The piles were made of hollow aluminum tubes closed at both ends. Each pile was 40.6 cm long of which 38.1 cm was embedded. The piles had varying diameters of 1.91, 3.02, and 5.08 cm and thickness of 0.10, 0.26 and 0.22 cm respectively.

DENSITY OF SAND BED

The model pile tests were performed in sand beds prepared in a steel tank measuring 61 cm x 61 cm x 61 cm. A loose sand bed and a dense sand bed were prepared. The density of the loose sand was 1.43 Mg/m^3 and that of the dense sand was 1.68 Mg/m^3 . The loose sand bed was prepared by discharging the sand through a hopper maintained at a fall height of 10.2 cm, and the dense sand bed was prepared by compacting the sand in layers.

PILE PLACEMENT AND LOADING

The model piles were placed under two different installation conditions. Under one condition, the piles were first placed in the steel tank which was then filled with sand. These were called non-displacement (or non-driven) piles. In another condition, the piles were driven after the sand was placed in the tank. These were called displacement (or driven) piles.

The model pile tests were done according to ASTM F1143-74. The piles were loaded through a proving ring and a gear box connected to a handle. A penetration rate of 0.08 to 0.25 cm/min was maintained during loading. The loading was continued till failure. Here, the failure load was identified as the load at which a small load increment caused a substantial pile head displacement.

TESTS USED IN THE ANALYSIS

In this study, model pile tests performed in the loose sand bed only are used. The loose sand bed had a density of 1.43 Mg/m^3 . Test results of both displacement and non-displacement piles are considered.

FINITE ELEMENT METHOD

The finite element procedure involves discretization of the pile using one-dimensional two-noded line elements. At each node, the line element has one degree of freedom corresponding to axial displacement. The resulting finite element equations are expressed as,

$$[K_t] \{\Delta q\} = \{\Delta Q\} \quad (1)$$

where, $[K_t]$ = tangent stiffness matrix, $\{\Delta q\}$ = incremental nodal displacement vector, and $\{\Delta Q\}$ = incremental nodal load vector.

In this study, the behavior of the pile material is assumed to be linearly elastic while that of the soil is assumed to be non linearly elastic. Thus, any non linearity introduced in the stiffness matrix is entirely due to the nonlinear responses of the soil springs modelled using the t-z and p-z concepts.

INCREMENTAL METHOD

A nonlinear incremental technique is used for the analysis of axially loaded piles. In this technique, the total load is divided into a number of increments and applied increment by increment. The stiffness matrix $[K_t]$ is updated at the end of each increment and used for the succeeding increment. For linear elastic analysis, the total load is applied in one increment.

DEVELOPMENT OF NONLINEAR SPRINGS

The proposed procedure involves finding of the t-z curves at different depths along the pile length and the p-z curve at the pile tip. The t-z curves are used to represent shear resistances, and the p-z curve is used to represent tip resistance.

t-z Curves

Kraft et. al. (1981) gave the detail description of the t-z curves. Here, only the salient features of these curves are described. The t-z (or shear-displacement) relation is described by a theoretical model based on the theory of elasticity. This theoretical model expresses pile displacement as function of the geometrical properties of pile and soil as,

$$Z_s = \frac{r_o}{G_i} \ln \frac{r_m/r_o}{1-\psi} \quad (2)$$

where Z_s = displacement of shaft element; t =shear resistance at pile-soil interface; r_o =pile radius; r_m = influence radius beyond which soil shear stress is zero= $2.5L\rho (1 - \nu_s)$; L =pile length; ρ =ratio of soil shear moduli at depths $L/2$ and L ; ν_s =Poisson's ratio of soil; $\psi=t R_f/t_{max}$; R_f = stress strain curve fitting constant for soil and this constant is defined as the ratio ultimate stress to the failure stress; t_{max} =soil shear stress at failure; G_i =initial shear modulus of soil= $E_i/2(1 + \nu_s)$; E_i =initial Young's modulus of soil. E_i is assumed to be a hyperbolic function of confining pressure (Janbu 1963) as,

$$E_t = K pa \left(\frac{\sigma_v}{pa} \right)^n \quad (3)$$

where pa = atmospheric pressure; σ_v = effective overburden pressure; K and n = hyperbolic constants. Here, t_{max} is assumed to be the limiting value of t at failure as,

$$t_{max} = K_h \sigma_v \tan \delta \quad (4)$$

where K_h = lateral earth pressure coefficient; δ = frictional angle of pile-soil interface. Having determined the parameters in Eq. 3 and 4, the t - z curve at any depth can be determined using Eq. 2. The t - z curve may then be used to predict the shear (t) for any pile displacement (z_s).

The t - z relation (Eq. 2) is used to calculate the initial stiffness of friction spring. The initial stiffness of t - z spring (k_{OS}) at any depth is taken as the initial slope of the t - z curve at that depth. Thus,

$$k_{OS} = \left. \frac{\partial z_s}{\partial t} \right|_{t=0} \quad (5)$$

p-z Curve

Randolph and Wroth (1978) gave the load-displacement (p - z) relation at pile tip as,

$$z_t = p_t \frac{(1-v_s)\eta}{4r_0G_1} \quad (6)$$

where z_t = tip displacement; p_t = tip load (per unit area); η = influence factor. Now the linear elastic stiffness of tip spring (k_b) may be expressed as,

$$k_b = \frac{p_t}{z_t} = \frac{DE_1}{(1-v_s)^2} \eta \quad (7)$$

where D = pile diameter. The appropriate value of $\eta=1$ was reported by Randolph and Wroth (1978) for long pile. However, in this study, this value did not provide good correlation with the observed behavior. It was found that $\eta=1$ significantly under-estimates the failure pile load and poorly predicts the load-deformation behavior. Hence, the initial stiffness of p - z spring (k_{Ot}) is assumed as,

$$k_{Ot} = \lambda k_b \quad (8)$$

where λ = constant. Armaleh and Desai (1987) suggested $\lambda = 2.6$ from pile load test results. In this study, this value of λ is adopted.

RAMBERG-OSGOOD MODEL

The proposed procedure utilized this model to simulate the nonlinear behavior of t - z and p - z springs. For the t - z spring, the model in the hyperbolic form may be expressed as,

$$t = \frac{(k_{OS} - k_{fs}) z_s}{(k_{OS} - k_{fs}) z_s} + k_{fs} z_s \quad (9)$$

$$1 + \left| \frac{p_{fs}}{p_{fs}} \right|$$

where k_{fs} = final stiffness of t - z spring; p_{fs} = shear load at failure. In this study, $k_{fs} = 0$ and $p_{fs} = t_{max}$ (Eq. 4) are assumed. Figure 1 shows a schematic of the model used in this study.

For the p-z spring, the model in the hyperbolic form may be expressed as,

$$P_t = \frac{(k_{ot} - k_{ft}) z_t}{1 + \frac{(k_{ot} - k_{ft}) z_t}{p_{ft}}} + k_{ft} z_t \quad (10)$$

where k_{ot} = initial tip resistance; k_{ft} = final stiffness of p-z spring; p_{ft} = tip load at failure. In this study, k_{ft} is taken as zero. For sand, p_{ft} is assumed as,

$$P_{ft} = q N_q \quad (11)$$

where q = effective overburden pressure at the tip; N_q = bearing capacity factor. A schematic of p - z curve is similar to that of the t - z curve shown in Fig. 1.

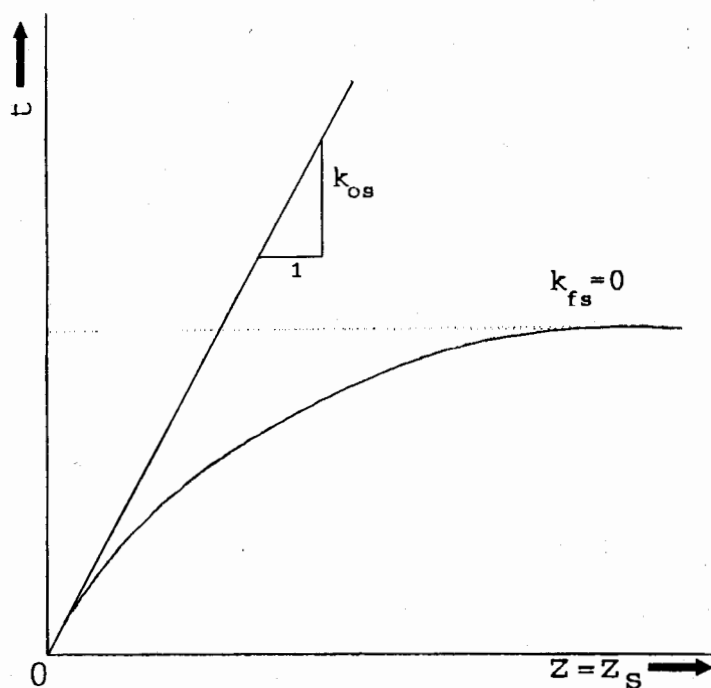


Fig 1. A schematic of t-z Curve

PILE AND SOIL PROPERTIES

For the analysis herein, the aluminum pile is assumed to be linearly elastic, and the sand is assumed to be non linearly elastic. Details of the parameters for pile and soil are given below:

Young's modulus of pile, E_p	= 55.2 GPa
Unit weight of sand, γ	= 1.43 Mg/m ³
Poisson's ratio of sand, ν_s	= 0.30
International friction angle of sand, ϕ	= 31°
Hyperbolic constant, K	= 120
Hyperbolic constant, n	= 1.03

The hyperbolic constants (K and n) are determined from triaxial tests performed at four different confining pressures of 380, 520, 690 and 1450 kPa (Morshed 1991). The earth pressure coefficient (K_h) and the bearing capacity factor (N_q) are estimated using the experimental results of Siddique (1988) for the 3.02 cm diameter pile. The results of the pile under both displacement and non-displacement conditions are used to get a set of K_h and N_q values for each installation condition. The following conventional equations for the total shaft load (Q_s), total tip load (Q_t) and total pile load (Q) are used.

$$Q_s = \frac{1}{2} \gamma L K_h \tan \delta A_s \quad (12)$$

$$Q_t = \gamma L N_q A_t \quad (13)$$

$$Q = Q_s + Q_t \quad (14)$$

where A_s = surface area of shaft; A_t = cross-sectional area of tip. In these equations, the effect of sand arching is neglected. Also, $\delta = \phi$ is assumed due to the absence of sufficient test data. For the 3.02 cm pile, Siddique (1998) reported $Q = 267$ N, $Q_t = 127$ N for the displacement pile and $Q = 200$ N, $Q_t = 111$ N for the non-displacement pile. Thus using Eqs. 12, 13 and 14, it has been calculated that $K_h = 2.45$ and $N_q = 34$ for displacement piles and $K_h = 1.45$ and $N_q = 29$ for non-displacement piles.

In Table 1, the above K_h values obtained using the conventional equations are compared with those suggested by Sowers and Sowers (1970). To use the values of Sowers and Sowers (1970), the relative density of soil (D_r) is needed. As D_r is not reported by Siddique (1988), the following equation (Meyerhof 1959) is used to determine D_r .

$$\phi = 28^\circ + 15^\circ D_r \quad (15)$$

Thus, for the sand used in this study having $\phi = 31^\circ$, the D_r is 20%. With this value of D_r , the K_h values are estimated by linear interpolation between $D_r = 0\%$ and $D_r = 50\%$.

Table 1. Comparison of K_h values

Installation condition	K_h values		
	Calculated ¹	Estimated ² $D_r = 20\%$	Sowers ³ $D_r < 50\%$
Displacement	2.45	2.45	2.00-3.00
Non-displacement	1.45	1.30	0.75-1.50

1. Using experimental results of Siddique (1988).
2. Using Sowers and Sowers (1970).
3. Taken from Sowers and Sowers (1970).

In Table 2, the N_q values calculated from experimental data using the conventional equations are compared with those suggested by Vesic (1967). It is noted that the Vesic's values do not consider installation condition. Hence, the value is same for both the installation conditions and appears to be the average of the N_q values for displacement and non-displacement conditions obtained by the conventional equations.

Table 2. Comparison of N_q values

Installation condition	N_q values	
	Calculated	Vesic (1967) $\phi = 31^\circ$
Displacement	34	32
Non-displacement	29	32

The parameters for $t - z$ curves are evaluated at each nodal point along the pile and those for $p - z$ curve are evaluated at the pile tip. Typical values for 3.02 cm diameter pile are given in Tables 3 and 4.

Table 3. $t - z$ Parameters for $D = 3.02$ cm Pile

Soil Depth cm	Displacement		Non-displacement	
	K_{os} N/cm^3	P_{fs} N/cm^2	K_{os} N/cm^3	P_{fs} N/cm^2
0.00	0.00	0.00	0.00	0.00
2.54	0.76	0.05	0.44	0.03
5.08	1.52	0.10	0.90	0.06
7.62	2.34	0.16	1.36	0.09
10.16	3.27	0.21	1.82	0.12
12.70	4.08	0.26	2.31	0.15
15.24	4.90	0.31	2.72	0.19
17.78	5.71	0.37	3.27	0.21
20.32	6.53	0.42	3.81	0.25
22.86	7.35	0.47	4.08	0.28
25.40	8.16	0.53	4.63	0.31
27.94	8.98	0.57	5.17	0.34
30.48	9.80	0.63	5.71	0.37
33.02	10.61	0.68	6.26	0.40
35.56	11.43	0.76	6.53	0.44
38.10	12.24	0.76	7.07	0.46

Table 4. p-z Parameters for D = 3.02 cm Pile

Soil Depth cm	Displacement		Nondisplacement	
	k_{ot} N/cm ³	Pft N/cm ²	k_{ot} N/cm ³	Pft N/cm ²
38.10	176.87	17.97	103.40	15.21

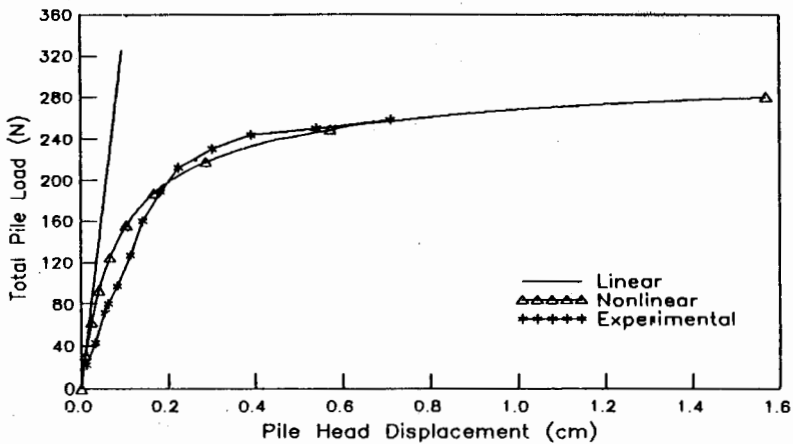
SELECTION OF FINITE ELEMENT MESH AND LOADING INCREMENT

A parametric study is performed to select an appropriate finite element mesh and a suitable loading increment (Morshed 1991). The 3.02 cm diameter displacement pile is discretized using 4, 10 and 16 equally spaced nodes. It is observed that satisfactory results may be obtained with 16 nodes. In order to select a suitable load increment for the nonlinear analysis, the pile is discretized using 16 nodes and analyzed using load increments of 22.25, 8.90 and 2.23 N. It is observed that satisfactory results may be obtained using a load increment of 2.23 N. Thus, for the present nonlinear analysis, the piles are discretized into 15 element with 16 nodes and the loads are applied using a load increment of 2.23 N.

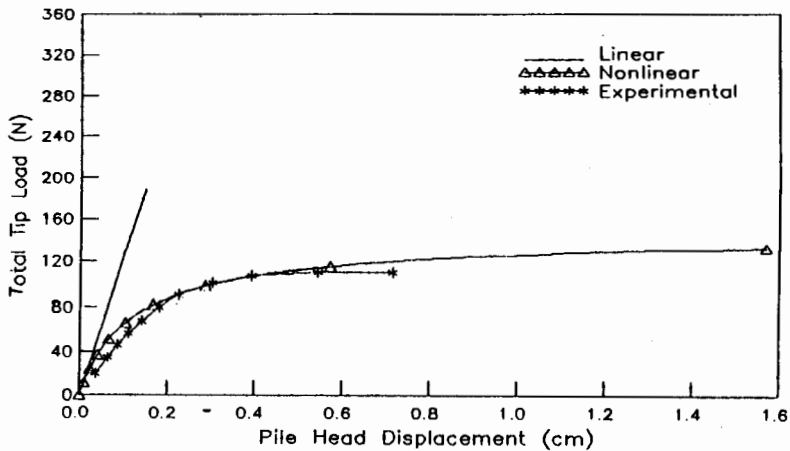
ANALYSIS AND INTERPRETATION OF RESULTS**Load-deformation behavior**

Displacement Piles : The analysis begins with the critical examination of the 3.02 cm diameter pile. Figure 2 (a) shows three load displacement curves at the pile head for linear elastic case, nonlinear elastic case and experimental observations. As observed from Fig. 2 (a), the linear analysis can predict the experimental observations only in the initial range of loading. This is probably due to the fact that the soil behavior in this range is essentially linear elastic. However, the prediction made by the nonlinear analysis is found to be excellent for the entire range of loading. Figure 2 (b) shows three curves of tip load versus head displacement for linear analysis, nonlinear analysis and experimental observations. Here, the nonlinear analysis is found to compare satisfactorily with the experimental observations.

For the 1.91 cm pile, Fig. 3 shows the load-displacement behaviors at the head and tip obtained using linear analysis, nonlinear analysis and laboratory test results. The figure shows that the nonlinear analysis satisfactorily predicts the laboratory test results.



(a)

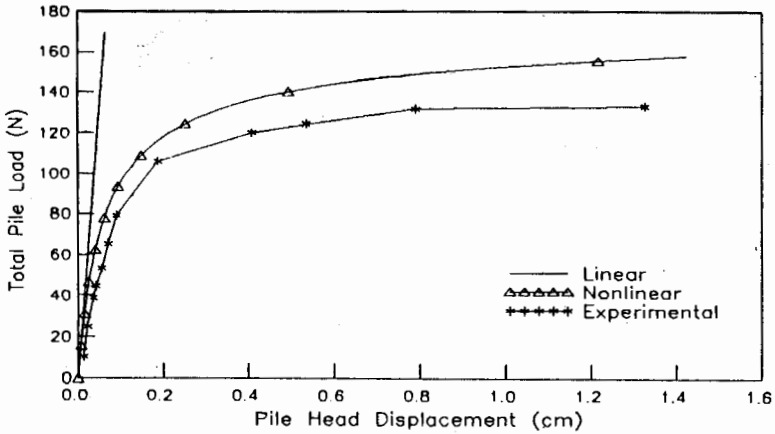


(b)

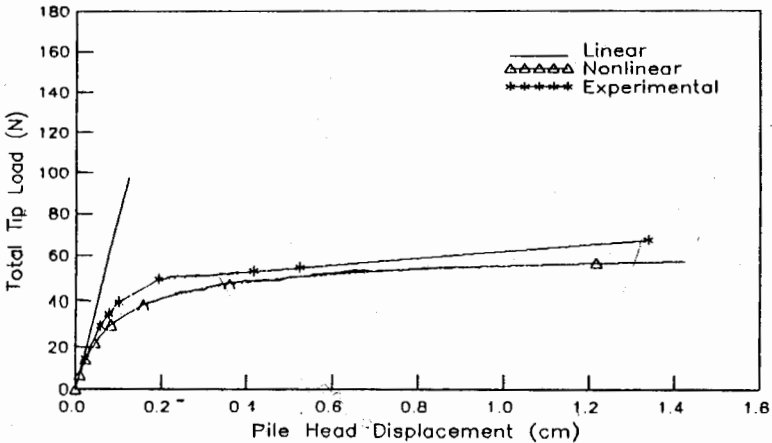
Fig 2. Load-Displacement Response of 3.02 cm Diameter Displacement Pile : (a) Pile Load versus pile Head Displacement; (b) Tip load versus pile Head Displacement.

For the 5.08 cm pile, Fig. 4 (a) shows that the predicted and the observed load-displacement behaviors at the pile head are comparable. However, Fig. 4 (b) shows that the comparison at the pile tip is not satisfactory. Here the experimentally observed value of the tip load appears to be significantly smaller than the predicted values. However by

observing the tip loads of the other two piles (Figs. 2 (b) and 3 (b)), it can be concluded that the experimental determination of the tip load for this particular 5.08 cm pile was erroneous. As the tip load of a pile is supposed to increase with its tip area, the tip load of 5.08 cm diameter pile should be about 3 times that of the 3.02 cm diameter pile and 7 times that of the 1.91 cm diameter pile, but this was not observed by Siddique (1988).

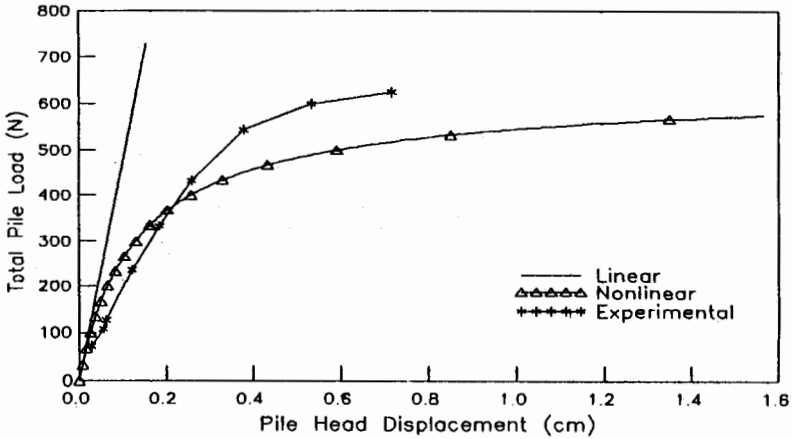


(a)

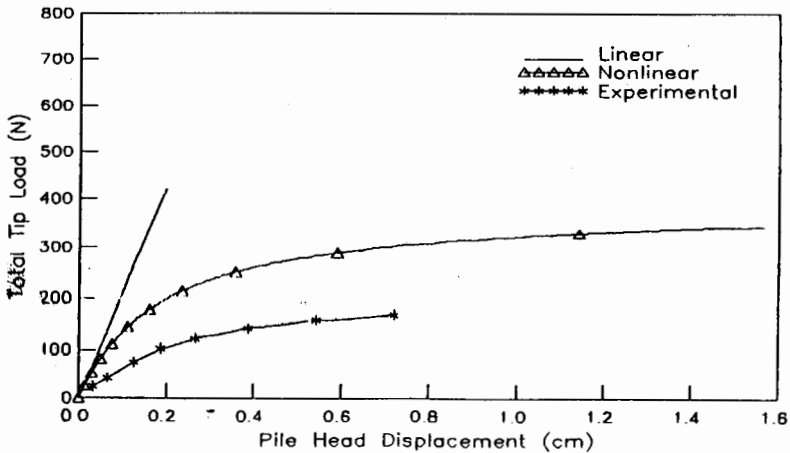


(b)

Fig 3. Load-Displacement Response of 1.91 cm Diameter Displacement pile : (a) Pile Load versus p pile Head Displacement; (b) Tip load versus pile Head Displacement.



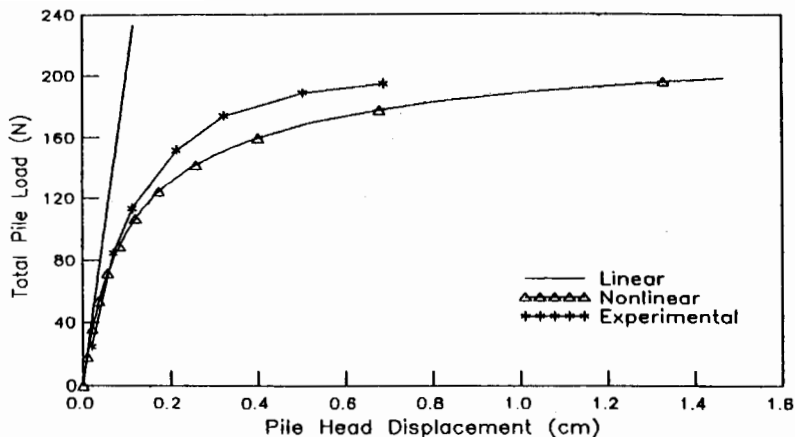
(a)



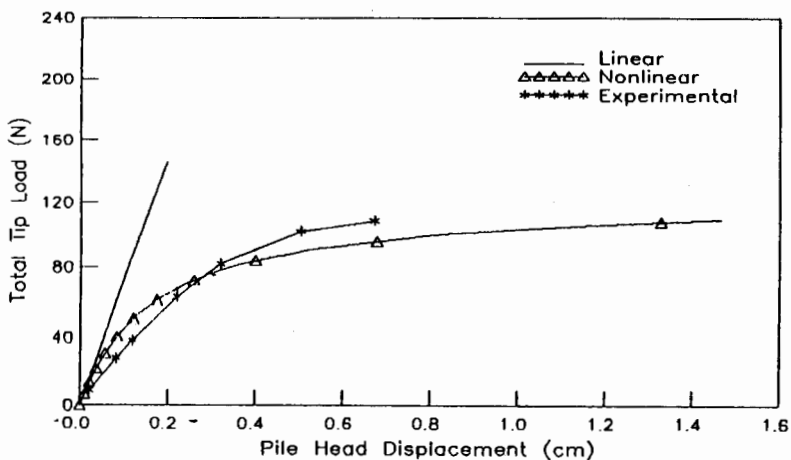
(b)

Fig 4. Load-Displacement Response of 5.08 cm Diameter Displacement pile : (a) Pile Load versus pile Head Displacement; (b) Tip load versus pile Head Displacement.

Non-displacement Piles : The predicted and observed load-displacement behavior of the non-displacement piles are shown in Figs. 5, 6 and 7. From all these figures, it again appears that the linear analysis can predict load-displacement behavior only in the initial range of loading. The predictions of load-deformation behaviors at the



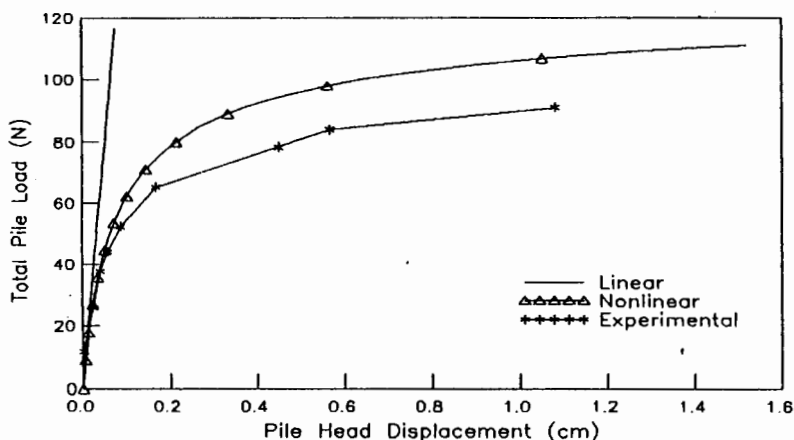
(a)



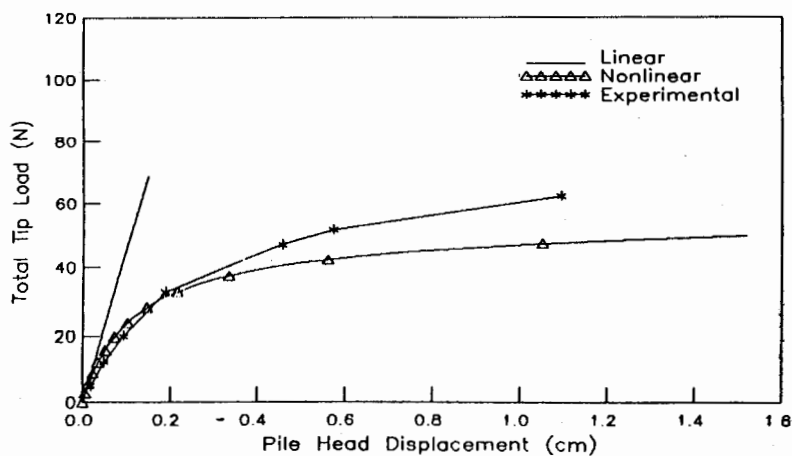
(b)

Fig 5. Load-Displacement Response of 3.02 cm Diameter Non Displacement pile : (a) Pile Load versus pile Head Displacement; (b) Tip load versus pile Head Displacement.

head and tip compare well for both the 3.02 cm and the 1.91 cm diameter piles (Figs. 5 and 6). For the 5.08 cm diameter pile, the load-deformation behavior at the pile head is also found to be quite satisfactory. However, the behavior at the tip could not be compared as Siddique (1988) did not report the required experimental observations.

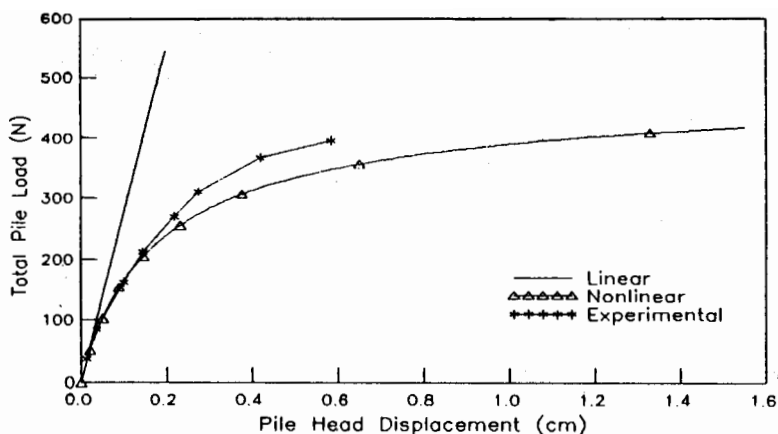


(a)

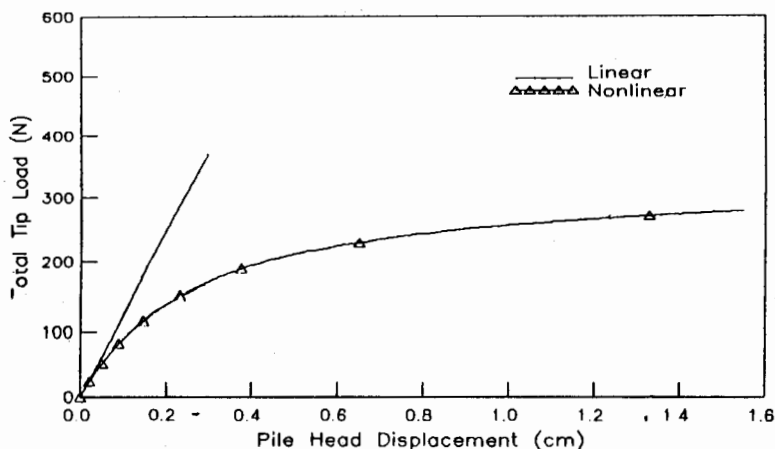


(b)

Fig 6. Load-Displacement Response of 1.91 cm Diameter Non-Displacement Pile : (a) Pile Load versus pile Head Displacement; (b) Tip load versus pile Head Displacement.



(a)



(b)

Fig 7. Load-Displacement Response of 5.08 cm Diameter Non-Displacement Pile : (a) Pile Load versus pile Head Displacement; (b) Tip load versus pile Head Displacement.

PREDICTION OF FAILURE LOADS

Failure loads for displacement and non-displacement piles predicted by nonlinear analysis are listed in Table 5. Also, included in the table are the failure loads observed experimentally and those calculated by conventional procedure (Eqs. 12, 13 and 14). Here, the failure load is identified as the load asymptotic to the load-displacement curve. From

the table it appears that the predicted loads compare well with the observed loads.

Table 5. Prediction of Failure Loads

Installation condition	Pile diameter (cm)	Failure loads (N)		
		Predicted	Observed	Estimated
Displacement	1.91	156	134	142
	3.02	267	267	271
	5.08	587	619	619
Non-displacement	1.91	107	93	98
	3.02	191	191	191
	5.08	401	401	454

For the 1.91 cm diameter displacement pile, the predicted failure load over-estimates the experimental and conventional values by 16% and 10% respectively. However, for the remaining two displacement piles, the comparisons are found to be highly satisfactory.

For the 1.91 cm diameter non-displacement pile, the predicted failure load over-estimates the experimental and conventional values by 15% and 9% respectively. However, for the 3.02 cm diameter pile, the comparison is found to be excellent. For the 5.08 cm diameter pile, the experimental and predicted failure loads compare extremely well. However, the predicted value under-estimates the conventional value by 12%.

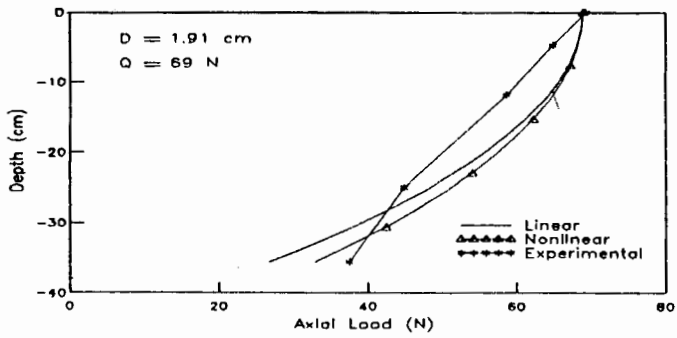
From the above discussion it appears that the failure loads predicted by the proposed numerical procedure is quite satisfactory. Also, the failure loads calculated by the conventional method of analysis compare satisfactorily with the observed and predicted values.

COMMENTS

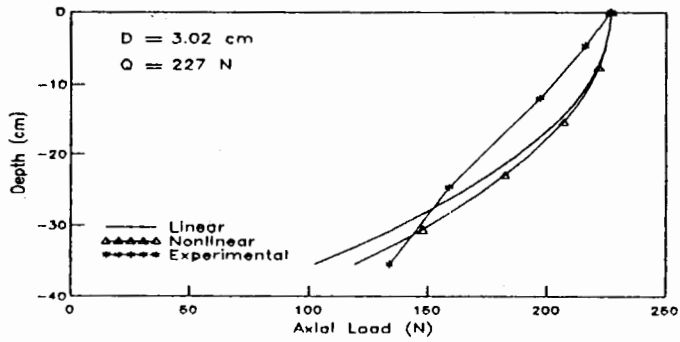
It is interesting to note that the best results are obtained for the 3.02 cm diameter pile. This is due to the fact that this pile has been used to estimate the lateral earth pressure coefficient and the bearing capacity factor in the present analysis. This also shows the applicability of the proposed method provided the necessary parameters are properly determined.

AXIAL LOAD DISTRIBUTION

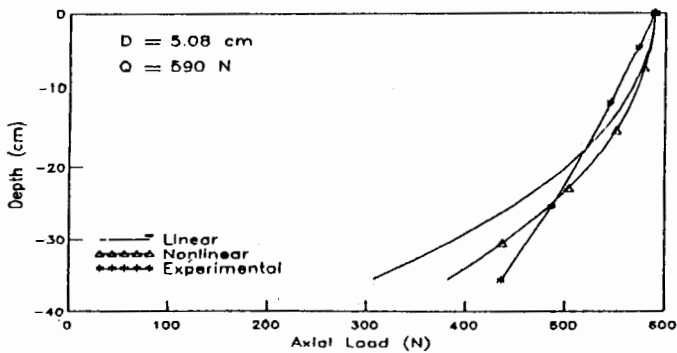
Figures 8 and 9 show the distribution of axial load along the pile length for various cases and for different pile load (Q) as reported by Siddique (1988). It should be noted that these pile loads do not necessarily correspond to the pile loads at failure. Figures 8 and 9 include results of linear analysis, nonlinear analysis and experimental



(a)

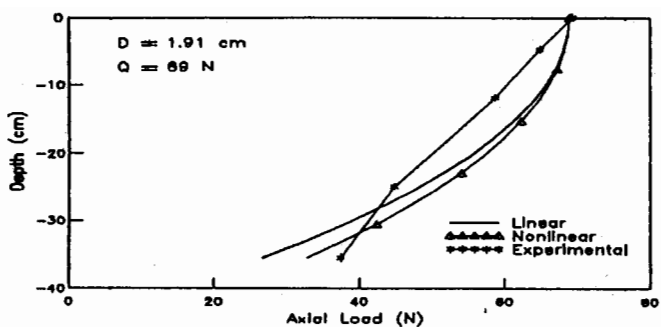


(b)

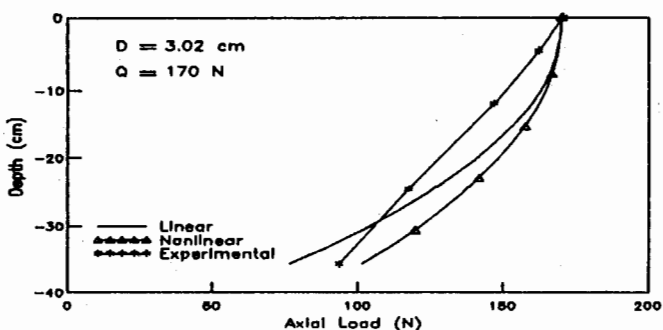


(c)

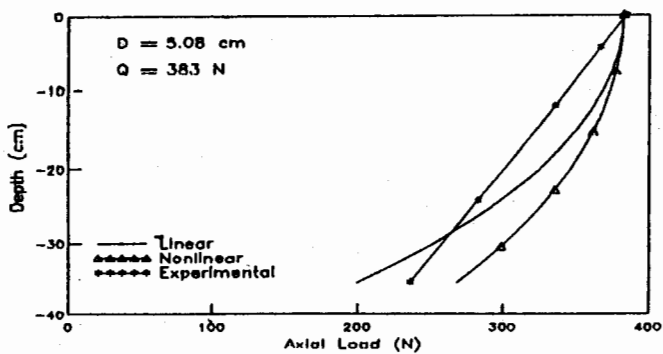
Fig 8. Axial Load-Distribution of Displacement piles for Different pile Diameters



(a)



(b)



(c)

Fig 9. Axial Load-Distribution of No-Displacement piles for Different pile Diameters

observations. It appears that the linear and the nonlinear analysis can satisfactorily predict the experimental axial loads. However, the magnitude of axial load at any depth obtained using the nonlinear analysis, appears higher than that obtained by the linear analysis. As load increases, the soil in the upper portion of the pile is subjected to more plastic deformation than that in the lower portion. Thus, the upper soil yields earlier and transfers more load to the lower soil. However, no such yielding is accounted in the linear elastic analysis. The pattern of numerical prediction for axial load distribution in all cases found to be parabolic in nature which contradicts with those of experimental observations. This may be due to error in measuring axial loads. Poulos (1979), Bhandari (1989) and Briaud, and Tucker (1989) reported parabolic distribution of axial load along the pile length.

CONCLUSIONS

A simple nonlinear incremental finite element procedure is used to predict the load-deformation behavior and hence, the failure load of an axially loaded pile in sand. Material nonlinearity of soil is included in this study.

Load-deformation behavior of three model piles of various diameters under two different installation conditions are studied. Load-displacement response predicted by the proposed method compares well with the experimental observations. It thus appears that the $t - z$ and $p - z$ concepts can be effectively used to determine the initial stiffness of soil springs along the pile length and at its tip respectively. The simple form of hyperbolic Ramberg-Osgood model is found suitable in capturing the nonlinear soil response of axially loaded piles.

The present study shows that the nonlinear soil response significantly changes the load-deformation behavior of axially loaded piles. A linear elastic analysis provides satisfactory results only in the initial range of loading and fails to predict the ultimate behavior. In contrast, the nonlinear procedure yields complete load-deformation histories of the entire pile-soil system; such histories are difficult to predict by other procedures. As a result, the nonlinear procedure provides an enhanced understanding of the behavior of axially loaded pile-soil system. The failure loads predicted by the proposed procedure also compare well with the experimentally observed values. The maximum discrepancy between the failure loads obtained using this procedure and those observed experimentally is of the order of 16%.

REFERENCES

Armaleh, S. H., and Desai, C. S., (1987). "Load-deformation response of axially loaded piles." *J. Geotech. Engrg. Div., ASCE*, Vol. 113, No. 12, pp. 1483-1500.

Bhandari, A. K. M. (1989)., "Fields Loading Tests on Instrumented Piles-Hazira Slug Catcher Project". Proceedings of the 12th Int. Conf. on Soil Mechanics & Foundation Engineering, Vol. 2, pp. 1185-1188, New Delhi, India.

Bariaud, J. L., and Tucker, L. M. (1989). "Axially loaded five pile group and single pile in sand". Proceedings of the 12th Int. Conf. on Soil Mechanics & Foundation Engineering, Vol. 2, pp. 1121-1126, New Delhi, India.

Desai, C. S., and Wu, T. H. (1976). "A general function for stress-strain curves". Proc. 2nd Int. Conf. for Numerical Methods in Geomechanics, Blacksburg, Va.

Janbu, N. (1963). "Soil compressibility as determined by oedometric and triaxial test". Proc. European Conf. for Soil Mechanics and Found. Engng., 1 Weisbaden, Germany, pp. 19-25.

Kraft, L. M., Ray, R. P. and Kagawa, T. (1981). "Theoretical $t - z$ curves". J. Geotech. Engrg. Div., ASCE, Vol. 107, No. 11, pp. 1543-1560.

Morshed, J. (1991). "Prediction of load-deformation behavior of axially loaded piles in sand". M.Sc. Thesis, Dept. of Civil Engineering, Bangladesh University of Engineering and Technology, Dhaka, Bangladesh.

Meyerhof, G. G. (1959). "Computations of sands and bearing capacity of piles". J. Soil Mech. and Foundation Div., ASCE, 85 (SM6), pp. 1-27.

Muqtadir, A., Shafiullah, M. M., and Siddique, A. (1990). "Behavior of axially loaded model piles in sand". PILETALK Int. 90, Jakarta, Indonesia.

Poulos H. G. (1979). "Settlement of single piles in nonhomogeneous soil". J. Soil Mech. Foundation Div., ASCE, Vol. 105, No. GT5, May, pp. 627-642.

Randolph, M. F., and Wroth, C. P. (1978). "Analysis and deformation of vertically loaded piles". J. Geotech. Engrg. Div., ASCE, Vol. 104, No. 12, pp. 1465-1487.

Siddique, S. A. (1988). "Experimental studies of model pile behavior in sand". M.Sc. Thesis, Dept. of Civil Engineering, Bangladesh University of Engineering & Technology, Dhaka, Bangladesh.

Sowers, G. B., and Sowers, G. F. (1970). "Introductory Soil Mechanics and Foundations". Macmillan, New York, 3rd Ed.

Vesic, A. S. (1967). "Ultimate loads and settlements of deep foundations in sand". Bearing Capacity and Settlement of Foundation, A. S. Vesic (Ed.), Duke University, Durham, North Carolina.

Winkler, E. (1867). "die Lehre von der Elastizitat and Festigkeit". Prague, Czechoslovakia.

NOTIONS

A_s	=	surface area of shaft
A_t	=	cross-sectional area of tip
D	=	pile diameter
D_r	=	relative density of soil
δ	=	frictional angle of pile-soil interface
η	=	influence factor
E_i	=	initial Young's modulus of soil
E_p	=	Young's modulus of pile
G_i	=	initial shear modulus of soil
γ	=	unit weight of soil
$[K_t]$	=	tangent stiffness matrix
K	=	hyperbolic constant
k_b	=	linear elastic stiffness of p-z spring
k_{fs}	=	final stiffness of t-z spring
k_{ft}	=	final stiffness of p-z spring
K_h	=	lateral earth pressure coefficient
k_{os}	=	initial stiffness of t-z spring
k_{ot}	=	initial stiffness of p-z spring
L	=	pile length
λ	=	constant
n	=	hyperbolic constant
N_q	=	bearing capacity factor
V_s	=	Poisson's ratio of soil
p_t	=	tip load
p_a	=	atmospheric pressure

p_{fs}	=	shear load at failure
p_{ft}	=	tip load at failure
ϕ	=	internal friction angle of soil
q	=	effective overburden pressure of soil at tip
Q	=	total pile load
Q_s	=	total shaft load
Q_t	=	total tip load
$\{\Delta q\}$	=	incremental nodal displacement vector
$\{\Delta Q\}$	=	incremental nodal load vector
r_m	=	influence radius beyond which soil shear stress is zero
ρ	=	ratio of shear moduli of soil at depths $L/2$ and L
r_o	=	pile radius
R_f	=	stress-strain curve-fitting constant for soil
σ_v	=	effective overburden pressure
t	=	shear resistance at pile-soil interface
t_{max}	=	soil shear stress at failure
z_s	=	displacement of shaft element
z_t	=	tip displacement